# Analysis of a Computational Benchmark for a High-Temperature Reactor Using SCALE

Sedat Goluoglu*
*Oak Ridge National Laboratory, P.O. Box 2008, Bldg. 5700,*
*Oak Ridge, TN 37831-6170*

## Abstract

Several proposed advanced reactor concepts require methods to address effects of double heterogeneity. In doubly heterogeneous systems, heterogeneous fuel particles in a moderator matrix form the fuel region of the fuel element and thus constitute the first level of heterogeneity. Fuel elements themselves are also heterogeneous with fuel and moderator or reflector regions, forming the second level of heterogeneity. The fuel elements may also form regular or irregular lattices. A five-phase computational benchmark for a high-temperature reactor (HTR) fuelled with uranium or reactor-grade plutonium has been defined by the Organization for Economic Cooperation and Development, Nuclear Energy Agency (OECD NEA), Nuclear Science Committee, Working Party on the Physics of Plutonium Fuels and Innovative Fuel Cycles. This paper summarizes the analysis results using the latest SCALE code system (to be released in CY 2006 as SCALE 5.1).

***KEYWORDS: OECD, NEA, HTR, SCALE, plutonium, uranium, thorium***

## 1. Introduction

Numerous advanced reactor fuel designs have features that enhance the importance of the resonance processing procedure in obtaining accurate results in a system analysis. For example, the fuel for a high-temperature gas-cooled reactor (HTGR) consists of a double-layered geometry with small, tri-isotropic (TRISO) fuel particles uniformly distributed in graphite within a heterogeneous fuel element (or sphere). The fuel particles are closely packed (0.5-mm fissile material surrounded by 0.25-mm-thick moderator shell) so that interactions between the particles as well as the slowing down within the graphite matrix cannot be ignored. The fuel element (or sphere) is small enough that the heterogeneity of the fuel and interstitial moderator is also important, and the fuel particles cannot be considered to lie in an infinite medium.

*Corresponding author; Tel. +1-865-574-5288, Fax. 865-576-3513, E-mail: goluoglus@ornl.gov

## 2. Benchmark Definitions

Analyses have been performed using the benchmark definitions [1] provided by the Organization for Economic Cooperation and Development, Nuclear Energy Agency (OECD NEA), Nuclear Science Committee, Working Party on the Physics of Plutonium Fuels and Innovative Fuel Cycles. The computational benchmark has five phases in which infinite arrays of $UO_2$, $PuO_2$ and $ThO_2$-$UO_2$ fuelled pebbles as well as $UO_2$ and $PuO_2$ fuelled pebbles in a high-temperature reactor are analyzed. Parameter values relevant to the benchmark phases that have been analyzed are given in Table 1. Due to differences in available analysis methodologies and corresponding limitations, the infinite array problems have been further divided into two sections: (1) a spherical outer boundary with reflective or white boundary conditions, and (2) a cubic outer boundary with reflective boundary conditions. The calculation results provided by various participants of the computational benchmark project are published in another paper [2] in the proceedings of this conference.

## 3. Method

CSAS and CSAS6 sequences of SCALE [3] with the 238-group cross section library, which has 148 fast groups and 90 thermal groups (below 3 eV), have been used in calculating the infinite multiplication factor ($k_{inf}$). For each problem, two sets of calculations have been performed using ENDF/B-V-based and ENDF/B-VI-based evaluations. Deterministic calculations have been performed with the XSDRNPM module of SCALE using the S8 quadrature. XSDRNPM is a one-dimensional (1-D), Discrete Ordinates code. Monte Carlo calculations have been performed using KENO V.a and KENO-VI modules of SCALE. In all cases, the cross sections have been resonance-shielded using the CENTRM/PMC/CHOPS modules of the SCALE code system. CENTRM solves the 1-D transport equation using point-wise cross sections to calculate the corresponding point-wise spectrum, over an energy range specified by the user (usually the resonance range). PMC uses the point-wise cross sections, the CENTRM-calculated point-wise spectrum, and the multigroup data (where point-wise spectrum is not calculated) and generates multigroup cross sections. Double heterogeneity is accounted for by first calculating the point-wise flux disadvantage factors for the particle-matrix unit cell and then using these factors to create the homogenized point-wise particle/matrix mixture cross sections. The homogenized point-wise cross sections are used on the second pass to create the final resonance-shielded multigroup cross sections that represent the fuel pebbles. This scheme is very rigorous and does not rely on calculating Dancoff factors as is the case for most other multigroup resonance processing codes. Lattice effects are approximated by using the white boundary condition. The flowchart of the CSAS code sequence execution is shown in Fig. 1. Note that the CSAS6 sequence is the same as CSAS sequence except the Monte Carlo code KENO-VI is executed at the end.

For $k_{inf}$ calculations, XSDRNPM calculations used white boundary conditions on a sphere (pebble), whereas KENO V.a and KENO-VI calculations used reflected boundary conditions on a cube that contains the sphere (pebble).

**Table 1:** Parameter values

| Fuel in kernel $UO_2$ | | | | | |
|---|---|---|---|---|---|
| Parameter | Unit | Value | | | |
| $UO_2$ fuel density | g/cm$^3$ | 10.4 | | | |
| Uranium enrichment (by mass $^{235}U/(^{235}U + ^{238}U)$ | % | 8.2 | | | |
| Fuel natural boron impurity by mass | ppm | 1 | | | |
| Fuel kernel radius | cm | 0.025 | | | |
| Coating materials | - | C | C | SiC | C |
| Coating thickness | cm | 0.009 | 0.004 | 0.0035 | 0.004 |
| Coating radii | cm | 0.034 | 0.038 | 0.0415 | 0.0455 |
| Coating densities | g/cm$^3$ | 1.05 | 1.9 | 3.18 | 1.9 |
| Fuel in kernel $PuO_2$ | | | | | |
| Parameter | Unit | Value | | | |
| $PuO_2$ fuel density | g/cm$^3$ | 10.4 | | | |
| Fuel natural boron impurity by mass | ppm | 1 | | | |
| Fuel kernel radius | cm | 0.012 | | | |
| Coating materials | - | C | C | SiC | C |
| Coating thickness | cm | 0.0095 | 0.004 | 0.0035 | 0.004 |
| Coating radii | cm | 0.0215 | 0.0255 | 0.029 | 0.033 |
| Coating densities | g/cm$^3$ | 1.05 | 1.9 | 3.18 | 1.9 |
| Fuel in kernel $^{233}U/^{232}Th$ mixed oxide | | | | | |
| Parameter | Unit | Value | | | |
| Fuel density | g/cm$^3$ | 10.4 | | | |
| $^{233}U$ enrichment (by mass $^{233}U/(^{233}U + ^{232}Th)$ | % | 7.48 | | | |
| Fuel natural boron impurity by mass | ppm | 1 | | | |
| Fuel kernel radius | cm | 0.012 | | | |
| Coating materials | - | C | C | SiC | C |
| Coating thickness | cm | 0.0095 | 0.004 | 0.0035 | 0.004 |
| Coating radii | cm | 0.0215 | 0.0255 | 0.029 | 0.033 |
| Coating densities | g/cm$^3$ | 1.05 | 1.9 | 3.18 | 1.9 |
| Pebble | | | | | |
| Parameter | Unit | Value | | | |
| Unit cell square pebble array pitch (cubical outer boundary) | cm | 6 | | | |
| Unit cell coolant outer radius (spherical outer boundary) | cm | 3.53735 | | | |
| Pebble diameter | cm | 6 | | | |
| Radius of fuel zone | cm | 2.5 | | | |
| Outer carbon coating thickness | cm | 0.5 | | | |
| Outer carbon natural boron impurity by mass | ppm | 0.5 | | | |
| Number of coated particles per pebble | - | 15000 | | | |
| Packing fraction of coated particles | % | 9.043 | | | |
| Graphite matrix density | g/cm$^3$ | 1.75 | | | |
| Graphite matrix natural boron impurity by mass | ppm | 0.5 | | | |
| Outer carbon coating density | g/cm$^3$ | 1.75 | | | |

**Figure 1**: Flow diagram of CSAS sequence for doubly heterogeneous cells.

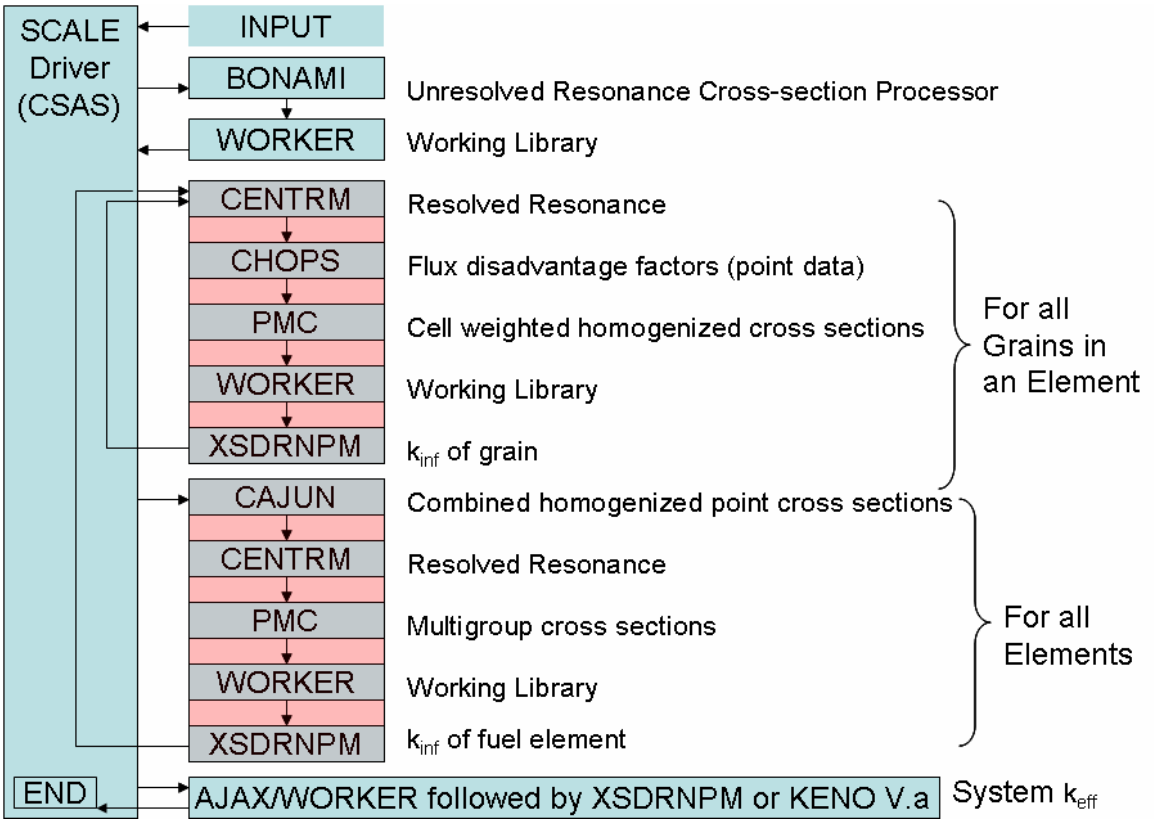


## 4. Results and Comparisons

Most of the results that have been provided to the organizers of the benchmark project are presented in another paper in this conference [2]. In this paper, only the computational results for infinite array problems for cold temperatures (293.6 K) are reported. Note that due to various improvements that have been recently made to the resonance processing modules CENTRM and PMC, the results in Ref. 2 are slightly different than those in this paper. In addition, results with cross sections that are based on the ENDF/B-VI evaluations are also provided in this paper.

The calculation results for the first, second, and fifth phases are listed in Tables 2 and 3 with ENDF/B-V and ENDF/B-VI cross sections, respectively. Analysis of the results shows that the impact of doubly heterogeneous resonance self-shielding is considerable for the $UO_2$-fuelled pebbles, with properly shielded cases calculating 8% higher $k_{eff}$ than homogenized cases. The effect of double heterogeneity is more severe for the case of plutonium in which the differences between simply homogenized and then resonance-shielded and properly resonance-shielded cases are as high as 20%. For thorium cases, on the other hand, there is not much difference between homogenized and doubly heterogeneous calculations. Similar trends were observed for high-temperature (1000 K) calculations as well (results are not included here, but are reported in Ref. [2]. For all cases with both sets of libraries, XSDRNPM, KENO V.a, and KENO-VI results

show excellent agreement with differences generally being less than two standard deviations of the Monte Carlo calculations. This is expected, because all three codes use the same resonance-shielded cross sections. Table 3 also shows the calculated values from MONK9 and MCNP (as reported in Ref. [2]). The $k_{inf}$ values calculated with KENO V.a and KENO-VI using ENDF/B-VI-based cross sections agree within 0.2% with MONK9 [4] results for plutonium and uranium/thorium systems. Comparison of $k_{inf}$ values between MONK9 and KENO codes, as well as MCNP [5] and KENO codes, is given in Table 4. The difference between the KENO codes and MONK9 is about 0.6% for uranium-only system. Comparison against MCNP shows a different trend where the KENO codes and MCNP are within 0.2% for uranium system and within 0.7% for plutonium system. Both MONK9 (with JEF2.2-based cross sections) and MCNP (with ENDF/B-VI cross sections) utilize continuous energy representation of the cross sections and, therefore, do not have to resonance-shield the cross sections. In contrast, the new capability in SCALE is used in generating properly resonance-shielded, multigroup cross sections.

**Table 2:** Effect of double heterogeneity with ENDF/B-V-based cross sections.

| ENDF/B-V-based cross sections | | | | | |
|---|---|---|---|---|---|
| Problem (phase) | Definition | Method | XSDRNPM | KENO V.a[(a)] | KENO-VI[(a)] |
| | | | $k_{inf}$ | $k_{inf}$ | $k_{inf}$ |
| 1 | Infinite array of $UO_2$-fuelled pebbles | Homogenized | 1.4033 | 1.4040 | 1.4034 |
| | | Doubly heterogeneous | 1.5109 | 1.5125 | 1.5157 |
| | | Difference, % | 8 | 8 | 8 |
| 2 | Infinite array of $PuO_2$-fuelled pebbles | Homogenized | 1.2205 | 1.2219 | 1.2210 |
| | | Doubly heterogeneous | 1.4629 | 1.4633 | 1.4629 |
| | | Difference, % | 20 | 20 | 20 |
| 5 | Infinite array of $UO_2/ThO_2$ fuelled pebbles | Homogenized | 1.4610 | 1.4610 | 1.4614 |
| | | Doubly heterogeneous | 1.4650 | 1.4643 | 1.4640 |
| | | Difference, % | 0.3 | 0.2 | 0.2 |

[(a)] Standard deviations for Problems 1 and 2 are less than 0.0005. Standard deviations for Problem 5 are less than 0.0003.

**Table 3:** Effect of double heterogeneity with ENDF/B-VI-based cross sections

| ENDF/B-VI | | | | | | JEF 2.2 | ENDF/B-VI |
|---|---|---|---|---|---|---|---|
| Problem (phase) | Definition | Method | XSDRNPM | KENO V.a[(a)] | KENO-VI[(a)] | MONK9[(b)] | MCNP[(b)] |
| | | | $k_{inf}$ | $k_{inf}$ | $k_{inf}$ | $k_{inf}$ | $k_{inf}$ |
| 1 | Infinite array of $UO_2$-fuelled pebbles | Homogenized | 1.4032 | 1.4037 | 1.4034 | | |
| | | Doubly heterogeneous | 1.5097 | 1.5139 | 1.5145 | 1.5222 | 1.5107 |
| | | Difference, % | 8 | 8 | 8 | | |
| 2 | Infinite array of $PuO_2$-fuelled pebbles | Homogenized | 1.2200 | 1.2211 | 1.2202 | | |
| | | Doubly heterogeneous | 1.4674 | 1.4671 | 1.4678 | 1.4657 | 1.4575 |
| | | Difference, % | 20 | 20 | 20 | | |
| 5 | Infinite array of $UO_2$/$ThO_2$-fuelled pebbles | Homogenized | 1.4615 | 1.4615 | 1.4617 | | |
| | | Doubly heterogeneous | 1.4648 | 1.4653 | 1.4646 | 1.4617 | -- |
| | | Difference, % | 0.2 | 0.3 | 0.2 | | |

[(a)] Standard deviations for Problems 1 and 2 are less than 0.0005. Standard deviations for Problem 5 are less than 0.0003.
[(b)] See Ref. [2].

**Table 4:** Comparison of $k_{inf}$ values

| Problem (phase) | Definition | Difference, %, MONK9 vs KENO V.a | Difference, %, MCNP vs KENO V.a | Difference, %, MONK9 vs KENO-VI | Difference, %, MCNP vs KENO-VI |
|---|---|---|---|---|---|
| 1 | Infinite array of $UO_2$-fuelled pebbles | 0.6 | -0.2 | 0.5 | -0.2 |
| 2 | Infinite array of $PuO_2$-fuelled pebbles | -0.1 | -0.7 | -0.1 | -0.6 |
| 5 | Infinite array of $UO_2$/$ThO_2$-fuelled pebbles | -0.2 | -- | 0.2 | -- |

## 5. Summary

A five-phase computational benchmark problem for an HTR has been modeled with SCALE version 5.1 (to be released in CY 2006) using the automated, user-friendly sequences CSAS and CSAS6. The XSDRNPM, KENO V.a, and KENO-VI results agree well, as expected, because they both use the same set of cross sections. The agreement with other Monte Carlo codes varies depending on the code and the system type (i.e., uranium-fuelled or plutonium-fuelled systems). The differences in the $k_{inf}$ values may be due to the cross section evaluations or to the different methods used (i.e., resonance processing and transport solution).

## References

1. G. Hosking and T. D. Newton, "Benchmark specification for an HTR fuelled with reactor grade-plutonium (or reactor-grade Pu/Th and U/Th): Proposal," NEA/NSC/DOC(2003)22, March 2005.
2. J. G. Hosking et al., "Analysis of an OECD/NEA High-Temperature Reactor Benchmark," Proc. of PHYSOR 2006, Vancouver, Canada, September 9-14, 2006.
3. "SCALE: A Modular Code System for Performing Standardized Computer Analysis for Licensing Evaluations," ORNL/TM-2005/39, Version 5, Vols. 1-3, April 2005. Available from Radiation Safety Information Computational Center at Oak Ridge National Laboratory as CCC-725.
4. N. R. Smith, M. J. Armishaw, and A. J. Cooper, "Current Status and Future Direction of the MONK Software Package," Proc. Int. Conf. on Nuclear Criticality Safety, ICNC2003, Tokai-mura, Japan, Oct. 20-24, 2003.
5. "MCNP: A General Monte Carlo N-Particle Transport Code, Version 4C," LA-13709-M, Los Alamos National Laboratory (2000).